

Central European Journal of Chemistry

Synthesis of terbium(III) complex with a biscoumarin derivative and its immobilization in PMMA-based composite thin films with fluorescent properties

Research Article

Denitsa K. Elenkova¹, Miroslava M. Getsova¹, Joana Ts. Zaharieva¹, Ilia Manolov², Maria M. Milanova^{1*}

¹Sofia University, Faculty of Chemistry and Pharmacy, Department of Inorganic Chemistry, 1164 Sofia, Bulgaria

²Medical University, Faculty of Pharmacy, Department of Organic Chemistry, 1000 Sofia, Bulgaria

Received 24 October 2012; Accepted 5 February 2013

Abstract: An amorphous complex of Tb(III) with the biscoumarin derivative 3,3'-[(4-hydroxyphenyl)methylene)]bis-(4-hydroxy-2H-1-benzopyran-2-one), Tb(H₂L)₃, was successfully synthesized and characterized. IR- and 'H-NMR- spectroscopy were used to investigate the coordination of the ligand around the Tb(III) ion. Values for the quantum yield and the life time of the excited state of the complex were obtained. The complex was immobilized in transparent and flexible PMMA-based films by a simple casting technique. PMMA/ chloroform solutions were used in synthetic procedures that resulted in both glass-supported and self-supporting nanocomposite films. The morphology of the films was studied by scanning electron microscopy, atomic force microscopy and transmission electron microscopy, showing the formation of crack-free films. The presence of the Tb(III) complex in the matrix was proven by the presence of characteristic bands in the IR spectra. Fluorescence microscopy and fluorescence spectroscopy demonstrated the promising optical properties of the films showing the characteristic emission bands of the Tb(III) ions. The longer life time of the excited state of the immobilized complex confirmed the protective role of the PMMA matrix on the optical properties of the complex. The composite films possessing optical properties have the potential for application as active components in optical devices.

Keywords: Tb(III) complex • Biscoumarins • Optical properties • Immobilization • PMMA matrix © Versita Sp. z o.o.

1. Introduction

1.1. Lanthanide complexes

Lanthanide ions, Ln(III), form complexes with organic ligands. These complexes have many applications, which are very often based on their optical properties. They are considered as active elements for OLEDs together with various organic molecules and metal-organic complexes; efficient OLEDs based on Tb(III) complexes have been reported [1]. The immobilization of the complexes in flexible, transparent matrices facilitates their application, especially for optical devices used in the visible and NIR area. Polymers doped with lanthanide complexes

have been investigated for optical amplification [2,3] and prototypes of flat panel displays containing lanthanide complexes have been presented [4,5]. Although, among the lanthanoids the Eu(III) ion is the most often explored luminescent ion in the visible light range with its typical red emission, the Tb(III) ion also has its interesting properties and advantages. Tb/Y mixed metal complexes have been tested as an emitting material in electroluminescence devices by immobilization in polyvinylcarbazole [6,7]; a complex of Tb(III) has been used for Eu(III) fluorescence enhancement in a PMMA matrix [8]; Tb(III) fluorescence in the green wavelength range of visible light has been studied for detection of bacterial

endospores in soil [9], for determination of carbofuran in water [10]; a Tb(III) complex has been designed to enhance formation of singlet oxygen [11] and for coupling of ${\rm Fe_3O_4}$ nanoparticles for magnetic resonance imaging applications [12]; ${\rm ZrO_2}$ -based fluorescent Tb(III) nanoparticles have been prepared as a fluorescent nanoprobe for time-resolved fluorescence bioassay [13]. Eu(III) and Tb(III) complexes with EDTA/o-phenanthroline have been proposed for the determination of these ions in presence of an excess of other Ln(III) ions [14]. Some Tb(III) complexes show luminescence that is sensitive to the oxygen concentration [15] so they may be applicable as oxygen sensors.

1.2. PMMA as a matrix for Ln(III) immobilization

The choice of poly(methylmethacrylate) as a matrix material is due to its good film-forming ability, transparency, mechanical strength and at the same time flexibility and low cost. It has been observed that the PMMA matrix acts as a co-sensitizer and enhances the luminescence intensity of the polymer films, providing UV protection for the luminescent species and thereby improving the photostability of the doped complexes [16]. Based on a PMMA matrix, films immobilized with different Ln complexes [16-22] have been prepared, showing that the applications of the complexes may be extended. Some problems have been identified [22] such as the difficulty to obtain a uniform distribution of the lanthanide complex in the polymer matrix as well as the low solubility of the lanthanide complexes in the polymer matrix

1.3. Coumarins, their Ln(III) complexes and the contributions of the present work

Benzo-α-pyrones or coumarins are a group of compounds consisting of fused pyrone and benzene rings, with the pyrone carbonyl group at position 2 (IUPAC name 2Hchromen-2-one, also known as 1-benzopyran-2-one) [23]. Recently, coumarin derivatives have attracted scientific interest because of the interesting properties these compounds possess, namely bioactivity and physiological properties [24-26]. On the other hand, their optical properties allow application as laser dyes, phosphorescent [27] and photochemical materials [28,29] and probes for heterogeneous systems using fluorescence spectroscopy [23]. Different Ln(III) complexes with coumarins such as those of La(III), Ce(III) and Nd(III) with 3,3'-benzylidene-bis(4-hydroxy-2H-1-benzopyran-2-one) [30] and those of Ce(III), Nd(III) [31] and Pr(III) [32] with coumarin-3-carboxylic acid have been synthesized and their spectral properties have been characterized. The crystal structures of complexes

of coumarin derivatives with Pr(III), Eu(III), Gd(III), Tb(III) and Er(III) have been investigated and the effect of the lanthanide radii on the structure and photoluminescence properties has been studied [33]. It has been found that both the optical [33] and biological [34,35] properties of the coumarins can be improved after coordination with different metal ions, especially with Ln(III) ions. Recently, new complexes of Ln(III) with coumarin derivatives were synthesized and characterized. The ligands used belong to a group of so called bis-coumarins, derivatives of 3,3'-benzylidene bis(4-hydroxy-2H-1-benzopyran-2-one), where some positions in the benzylidene ring are substituted by -OH, -NO2, CH2O-, -CI etc. Our experiments show that the substituent does influence the properties of the respective coumarin. The Tb(III) complexes prepared show optical properties that are promising if they can be transferred to a composite after their immobilization in a matrix.

The research presented here was done because the immobilization of these complexes can expand their potential practical application. The immobilization in a PMMA matrix of the Tb(III) complexes synthesized with the ligand H_3L , $C_{25}H_{16}O_7$, coumarin derivative 3,3'-[(4-hydroxyphenyl)methylene]bis-(4-hydroxy-2H-1-benzopyran-2-one), was attempted. The ligand H_3L contains an OH- substitute on the *para*-position and can react *via* one of the three available deprotonated OH-groups (Fig. 1).

The complex synthesized and presented here is the only one among several Tb(III) complexes obtained with H_3L having a good solubility in ethanol. This is very significant for the immobilization procedure in the matrix.

2. Experimental procedure

2.1. Materials

All the chemicals for the experiments were analytical grade. Poly(methylmethacrylate) (PMMA, Sigma Aldrich) (Mw = 90 000), chloroform (> 99.9 %, Sigma-Aldrich) as PMMA solvent and ethyl alcohol (Merck) as TbL10 solvent were used.

2.2. Preparation of the complex

The first step of the synthetic procedure was the deprotonation of the ligand by reaction with a base (sodium hydroxide) in a 1:1 stoichiometric ratio. As already shown [30], this leads to the formation of a sodium salt of the ligand in a water solution; the water solution of the Tb nitrate was added later on. The Na salt (salt of weak acid/strong base) is easy to hydrolyse;

Figure 1. Formula of 3,3'-[(4-hydroxyphenyl)methylene]bis-(4-hydroxy-2H-1-benzopyran-2-one), H_aL, with numbered carbon atoms.

this has to be taken into account because the ligand produced *via* hydrolysis can sometimes contaminate the substance obtained. The equations of the process are as follows:

$$H_3L + NaOH \rightarrow Na^+ + H_2L^- + H_2O$$
 $3H_2L^- + Tb^{3+} \rightarrow Tb(H_2L)_3$

According the procedure, to a suspension of 3 mmol (1.2852g) of the ligand in water, 3 mmol NaOH (0.12g) as a 0.1 M water solution was added while stirring. The red-colored sodium salt, soluble in water, was formed and the pH value of the solution was about 5. Then a water solution of 1mmol Tb(NO₃)₃ (0.3449g) was added: the formation of a precipitate with a light pink color was observed and the pH decreased to about 4.2. The suspension was stirred for about 2 hours and heated to 70°C. The precipitate was filtered, washed with hot water and dried. In order to remove any free ligand left in the sample, it was purified by dissolving it in ethanol; the solution was then filtered through a membrane filter and the ethanol evaporated at 40°C until a solid phase was formed.

2.3. Preparation of the films

To incorporate the Tb(III) complex synthesized into the polymer, the conventional method described in [17] was applied, namely direct dissolution of complex in the PMMA solution. The concentration of the complex in the immobilization matrix was varied in order to find out how it influences the fluorescent properties of the composite considering the potential self-quenching observed at higher concentrations of the lanthanide ion. However, it was found that the concentration of the complex cannot be increased very high because of its precipitation after solvent evaporation. The PMMA (0.2 g) was added to

CHCl $_3$ (4 mL) with stirring (400 rpm) at room temperature to create a transparent solution. The Tb(III) complex was dissolved in C $_2$ H $_5$ OH (1.5 mL) and added to the PMMA solution so that complex concentrations of 5, 7, and 10 wt.% in the PMMA matrix were obtained. After stirring for 60 min at room temperature, the final solution was cast on a glass plate, followed by drying at room temperature for 48 h. Self-supporting Tb(III) complex-PMMA nanocomposite films were peeled from the glass plate and characterized.

The Tb(III) complex/PMMA/CHCl $_3$ solution obtained was also used for deposition of thin films on glass substrates by dip coating. A withdrawal speed of 4 mm s $^{-1}$ was found to be optimal. PMMA films with 5, 7, and 10 wt.% TbL10 complex were prepared.

2.4. Characterization of the complex and the films

Elemental analysis. The content of C and H were determined by organic elemental analysis. The content of terbium was determined in ethanol media complexometrically as well as thermogravimetrically.

Scanning electron microscopy (SEM, JEOL, JSM-5510) was used to analyze the morphology of the films. To enhance the conductivity of the sample, a layer of gold was sputtered.

High resolution transmission electron microscopy (HRTEM) images were obtained with a JEOL JEM-2100 electron microscope operating at 200 kV.

Atomic force microscopy (AFM) images were recorded on a Veeco MultiMode system with a silicon cantilever using a taping mode.

Photoluminescence measurements of the films were made on a Cary Eclipse spectrometer with a xenon lamp as the excitation source as well as on an N-400M fluorescence microscope. The excitation spectra were monitored at 545 nm. The lifetimes of the excited state

of the complex obtained were averaged over at least three measurements.

Quantum yield measurements were performed on a Horiba Jobin Yvon Fluorolog 322 spectrometer equipped with visible light detection. The instrument was fitted with an integration sphere for the recording of absolute quantum yields on solution and solid-state samples.

Infrared (IR) spectra were recorded in the range 4000 cm⁻¹- 400 cm⁻¹ with a resolution of 1 cm⁻¹. To obtain spectra of the glass supported films, samples were taken from the support by scratching.

¹H–NMR spectra were recorded at room temperature on a Bruker Advance II+600 (600 MHz) spectrometer in DMSO-d_e. Chemical shifts are given in ppm.

3. Results and discussion

3.1. The complex $Tb(H_2L)_3 \cdot 5H_2O$ 3.1.1. Composition

The composition of the complex synthesized was determined by organic elemental analysis, by complexometric titration and by thermogravimetric determination of the metal. Elemental analysis were as follows (wt%): C (58.83/58.21), H (3.62/3.56), Tb (10.38/10.88). Based on these results, the formula $\text{Tb}(C_{25}H_{15}O_7)_3$:5 H_2O was suggested, which can also be presented as $\text{Tb}(H_2L)_3$:5 H_2O , where $H_2L=(C_{25}H_{15}O_7)$; later in the text it will be presented as TbL10. The sample is amorphous and attempts to obtain a single crystal failed so far. This is why the main information about the coordination of the ligand molecules around Tb(III) ion is based on IR- and 1H -NMR- spectroscopy.

3.1.2. Comparison of IR spectra of H₃L and Tb(III) complex

The important absorption bands to be considered are in the interval 3600-2000 cm⁻¹ and 1700-1200 cm⁻¹. The IR spectra of the ligand H₃L and the complex TbL10 in the interval 3600-2000 cm⁻¹ are shown in Fig. 2a. The synthetic procedure included a single deprotonation step; the anionic form of H₂L² obtained reacted with the Tb(III)-ions. The weak to medium bands due to the O-Hstretching mode in 4-hydroxy biscoumarin (3074 and 2924 cm⁻¹, Fig. 2a, 1) show a decreased intensity in the spectrum of TbL10 (one deprotonated OH) (Fig. 2a, 2). The bands observed at 2732 and 2608 cm⁻¹ are due to the presence in the ligand's OH groups participating in O-H-O intramolecular bonds (Fig. 2a, 1), which are not observed in the spectrum of the Tb(III) complex (Fig. 2a, 2). The symmetric and antisymmetric OH-stretching of the coordinated water (interval 3550-3200 cm⁻¹) [36] show a maximium around 3400 cm-1 in the spectrum of TbL10 (Fig. 2a, 2). The formation of stable C=O--H-bridges is cause for the very strong lowering of the C=O-stretching band to 1662 cm⁻¹ in the IR spectrum of the ligand H₂L (Fig. 2b, 1). The complex formation is causing changes in the 1700-1350 cm⁻¹ interval (Fig. 2b, 2). The band at 1662 cm⁻¹ does not occur in the spectrum of the complex, which is in agreement with the literature data [30] and is evidence for the coordination of the carbonyl groups. At the same time two new absorption bands with maxima at 1624 cm⁻¹ and 1599 cm⁻¹ appear. The band at 1624 cm⁻¹, corresponding to the plane deformational H₂O-vibrations, are due to crystal water molecules. The later is supported by the elemental analysis data. The characteristic vibration band for the Tb(III) coordination to C=O is the one at 1599 cm⁻¹ (antisymmetric stretching of C=O); the shoulder at 1621 cm⁻¹ can be considered as the symmetric stretching of C=O. The coordination of the ligand molecules to Ln(III)-ions through the carbonylic oxygens is also reported [30] for similar bis-coumarin derivatives.

3.1.3. ¹H-NMR – spectroscopic evidence for the formation of Tb(H,L)₀•5H₀O

Integrating the signals in the ¹H-NMR spectrum of H₂L shows the presence of 13 of the expected 16 protons (Fig. 3, lower curve). Apparently, the protons belonging to OH groups are not visible. At the left side of the spectrum a signal appears that suggests the presence of mobile protons. The only way to distinguish those protons is by connecting them with strong H-bonds or through decreasing their mobility by coordination. Indeed, the ¹H-NMR spectrum of Tb(H₂L)₃•5H₂O (Fig. 3, upper curve) shows 14 protons, i.e., a new signal from one of the non-deprotonated OH groups appeared. This is due to the coordination of the metal ion to H_aL. However, the paramagnetic behavior of Tb(III) present in the sample prevents the acquisition of two-dimensional spectrum (connecting ¹H- and ¹³C-, HMQC) that would have identified the OH group responsible for the signal at 9.04 ppm (left side of the spectrum, Fig. 3, up). The signal observed at 9.04 ppm is due to the coumarin OH group, because the metal ion coordinated close to that group is diminishing its mobility. The comparison of ¹H- NMR spectra of H₃L and of Tb(H₂L)₃•5H₂O shows shifting in the spectrum of the complex (Fig. 3, up).

3.1.4. Optical properties of Tb(H,L), • 5H,0

The absorption spectrum of powdered $Tb(H_2L)_3$ *5 H_2O in the ultraviolet region (210–350 nm) was obtained (Fig. 4a, 1); the absorption band is broad with a maximum at around 305 nm. The excitation spectrum for the complex recorded by monitoring

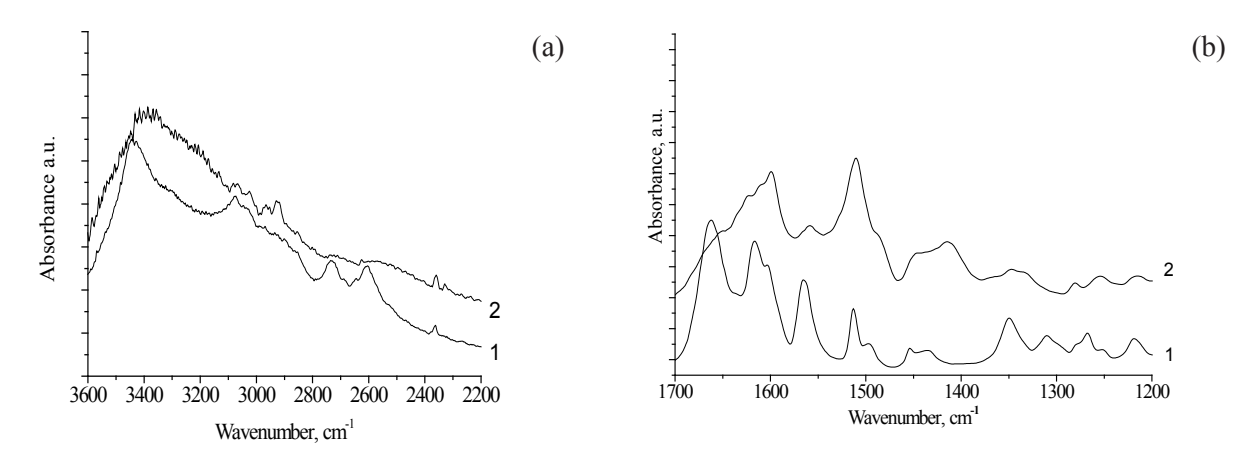


Figure 2. IR spectra of H₃L (1) and of Tb(III) complex (2) in the interval 3600-2000 cm⁻¹ (a) and 1700-1200 cm⁻¹ (b).

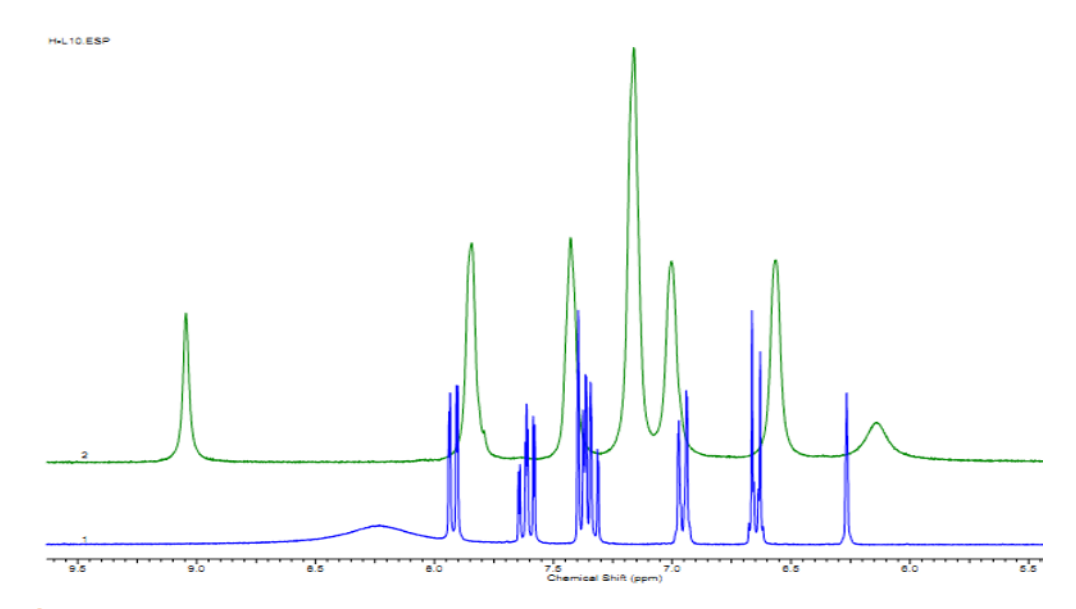


Figure 3. 1H- NMR spectra of H₃L (lower curve) and Tb(H₃L)₃•5H₃O (upper curve)

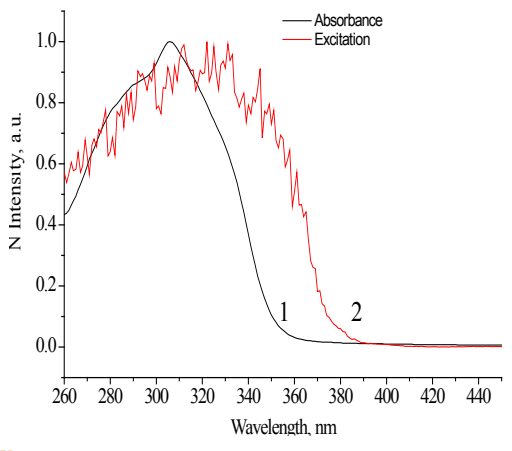
the Tb(III) luminescence at 545 nm in the range of 260–440 nm is shown in Fig. 4a, 2. The shift of the excitation peak relative to the absorption peak is about 20-30 nm.

When comparing the absorption spectra of a powdered sample and of a sample in ethanol solution, recorded in the range 210 – 440 nm, (Fig. 4b, 1 and 2) a minor red shift (about 15 nm) is observed in the spectrum of the powdered sample.

The emission spectra of a powdered sample and of a sample in ethanol solution at excitation wavelength $\lambda_{\rm ex}$ of 350 nm were recorded in the range 350 – 650 nm (Fig. 4b, 1 and 2). Ignoring the very weak plateau at around 400 nm, an emission band from the ligand was not observed, indicating efficient energy transfer to the Tb(III) ion. Tb(III) exhibits a green luminescence with the transitions of $^5D_4 \rightarrow ^7F_J$ (J=6-3). The

most intensive transition band ${}^5\mathrm{D}_4 \rightarrow {}^7\mathrm{F}_5$ at 545 nm is very intense and narrow, and is considered as a good probe for the ion [37]. The transition ${}^5\mathrm{D}_4 \rightarrow {}^7\mathrm{F}_2$ (in the region 640-655 nm) is a weak one [38] and is not observed here. Both emission spectra do not differ in the location of the emission peaks but there is a small difference in the intensity, which is more clearly seen for the transition ${}^5\mathrm{D}_4 \rightarrow {}^7\mathrm{F}_6$ (environmentally sensitive) [38]. The slight splitting in the structure observed may be due to nonequivalent Tb(III) sites [37] (Fig. 4b, 1 and 2) and the inhomogeneous environment of Tb(III) [38].

The lifetime of the excited state obtained for the TbL10 complex in a 0.001 M ethanol solution was 392 μ s, with a quantum yield of 7.4 \pm 0.2%; for a powdered sample of the same complex a shorter life time of 174 \pm 5 μ s and a lower quantum yield of 1.21 \pm 0.07% were obtained. The lower life time obtained for the powdered sample is



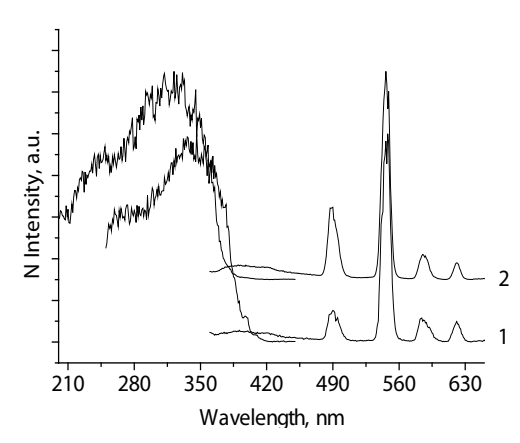
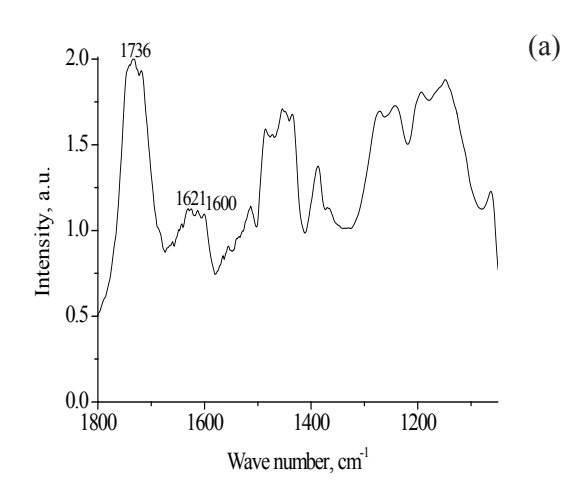


Figure 4. Absorption (a, 1) and excitation (a, 2) spectra and absorption/emission spectra of the powdered Tb(III) complex (b, 1) and of the complex dissolved in ethanol (b, 2) at λ_ω 350 nm. All the transitions start from the ⁵D₄ state and end at the ⁷F₁ levels (J = 6-3).



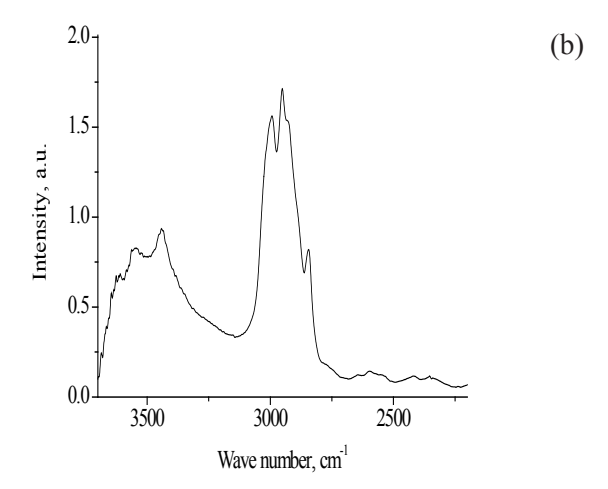


Figure 5. IR spectra of TbL10/PMMA self-supporting nanocomposite film (5%) in the range 1800-1000 (a) and 3750-2200 cm⁻¹ (b).

probably due to partial self quenching of the molecules of the complex. No similar literature data were found for Tb(III) complexes with 4-hydroxy- biscoumarins.

3.2. The films

3.2.1. IR-spectral evidence for the immobilization of TbL10 in the PMMA matrix

As was expected, the IR spectra show the characteristics of both complex and PMMA. The IR spectrum of TbL10/PMMA self-supporting nanocomposite film (5 wt.%) shows an absorption band at 1730 cm⁻¹, which is the most characteristic band for the C=O of a free ester and is due to the presence of PMMA (Fig. 5a). The overlapping bands in the interval 1620-1600 cm⁻¹ are typical for complexes of Ln(III) with 4-hydroxy coumarin derivatives [30-32], observed in the IR spectrum of Tb(H₂L)•5H₂O as well.These bands confirm the presence of the complex in the nanocomposite film. The absorption bands at 1600 cm⁻¹ (antisymmetric stretching

of C=O coordinated with Tb(III) ion), as well as the band at 1621 cm $^{-1}$ prove the participation of the C=O carbonyl group of the ligand $H_{\rm 3}L$ in coordination with the Tb(III) ion. In the spectral range mentioned, a deformation vibration of $\delta_{\rm H2O}$ can be seen; the presence of water is also indicated by the broad band at 3250-3500 cm $^{-1}$ (Fig. 5b).

The IR spectra of TbL10/PMMA nanocomposite films (5 and 7%) are compared in Fig. 6 in the very narrow range of 1800-1500 cm⁻¹. The characteristic vibration band for the Tb(III) coordination to C=O at 1599 cm⁻¹ becomes more intense when the concentration of the complex is increased.

Comparison of the spectra proves the successful incorporation of TbL10 into the PMMA matrix without structural modification. The other bands not commented are due to absorptions of the organic parts of the molecules and are not important for the immobilization behavior of the complex. The fact that the evident

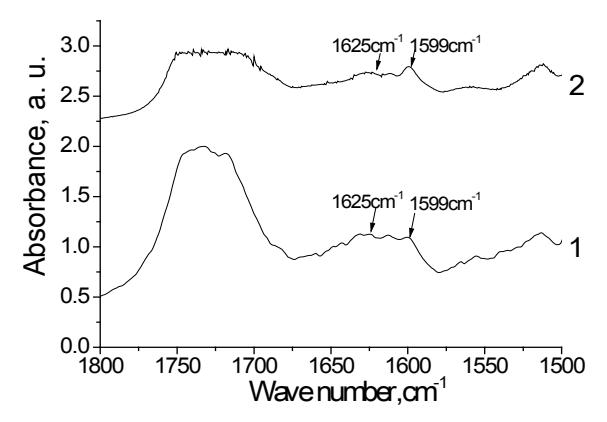


Figure 6. IR spectra of TbL10/PMMA nanocomposite films in the range 1800-1500 cm⁻¹, 5% (1) and 7% (2).

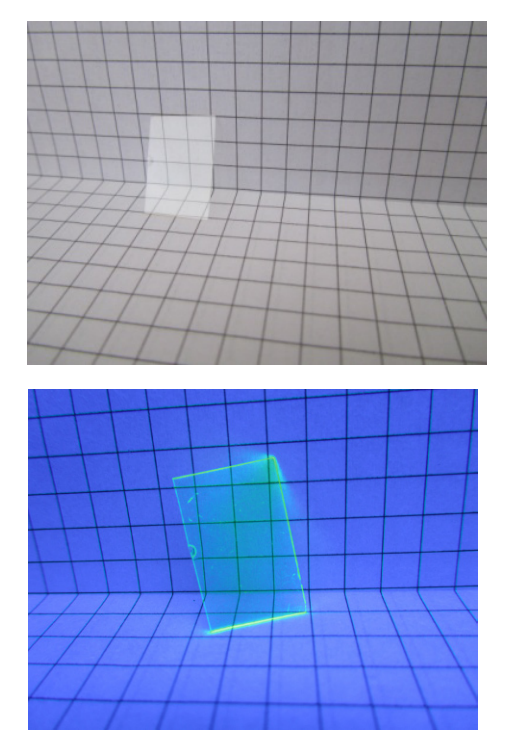


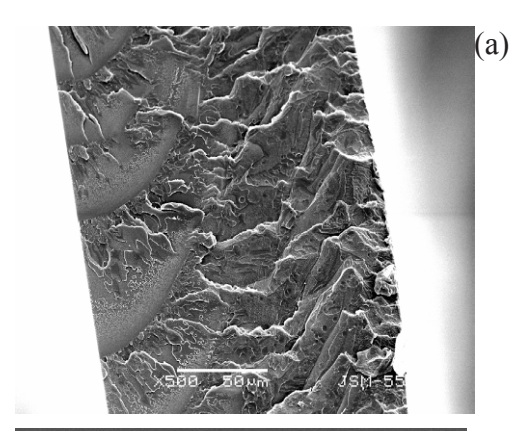
Figure 7. Photographs of transparent flexible TbL10/PMMA self-supporting nanocomposite film (5 wt.%) before (a) and after UV light exposure (b).

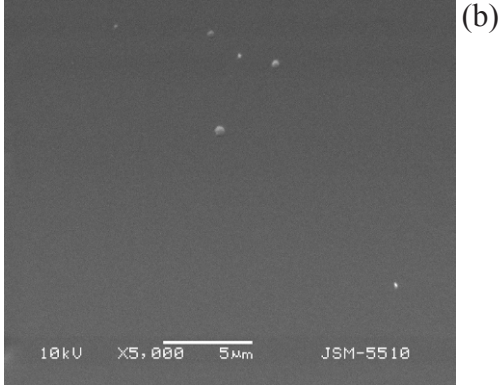
characteristic vibration bands related to the complex appear somewhat weaker in the IR spectra could be due to the low concentration of the complex.

IR spectra of TbL10/PMMA films on glass were found to be identical to those of the self-supporting film.

3.2.2. Distribution and morphology of TbL10 on selfsupporting films

Self-supporting transparent and flexible TbL10/PMMA nanocomposite films with dimension of 1.5×2 cm and thickness of approx. 200 μ m were prepared. The size of





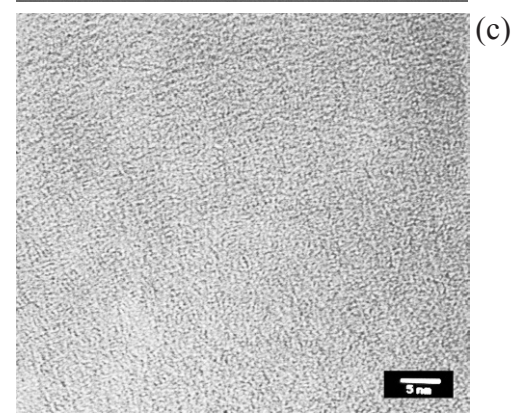


Figure 8. SEM micrographs with a different magnification ×500 (a) and ×5000 (b) and TEM micrograph (×1200000) (c) of TbL10/PMMA self-supporting nanocomposite film (5 wt.%).

the films is ultimately limited only by the dimension of the substrate. The uniformity of the films is demonstrated by the homogeneous green light emitted (Fig. 7) after irradiation with UV light.

A low-magnification SEM image of the self-supporting TbL10/PMMA film is shown in Fig. 8a, where a surface without cracks and microholes is visible; the densely-packed microstructure of the nanocomposite film is confirmed by the high magnification SEM image (Fig. 8b), as well as by TEM (Fig. 8c). On the TEM micrograph, strongly contrasted nanosized particles

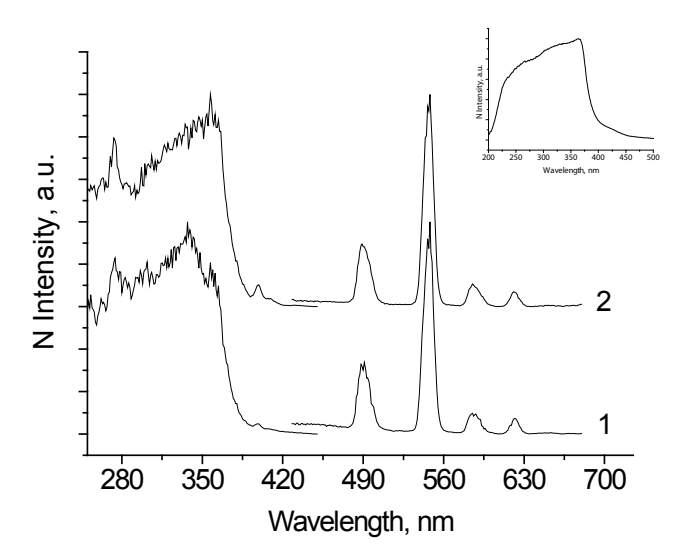


Figure 9. Absorption (inset), excitation and emission spectra for nanocomposite self-supporting TbL10/PMMA films, 5 (1) and 10 (2) wt.%. The excitation wavelength λ_∞ for the emission spectra was 350 nm. All transitions start from ⁵D₄ state and end at the ⁷F₁ levels (J = 6-3).

and short chains are visible that are probably TbL10 particles. The polymer chains of PMMA have probably set the pattern for formation of chains of the complex TbL10.

3.2.3. Optical properties of nanocomposite selfsupporting films

The absorption spectra of nanocomposite self-supporting TbL10/PMMA films (5 and 10 wt.%) do not differ, so only one of them is shown in the inset of Fig. 9. The excitation spectra were recorded at room temperature in the spectral range of 225 to 450 nm, by monitoring the emission at 545 nm (Fig. 9). The excitation spectra are dominated by the broad band in the region of 250 to 400 nm, which is due to absorption of the complex. The maxima of excitation are around 340-360 nm. The emission spectra recorded after excitation at 360 nm show 4 emission bands in the spectrum of the pure complex that are assigned to the characteristic inner shell transitions ${}^5D_4 \rightarrow {}^7F_1$ (J = 6-3) of the Tb(III) ion from the excited level to the lower levels. The pure TbL10 and the self-supporting films have the same number of emission lines. The slight splitting of the structure observed in the spectrum of the pure complex is also observed here. Some very weak emission of the ligand is noticeable at around 400-420 nm. The lifetime of the excited state of TbL10 in PMMA self supporting films was found to be 761.7 \pm 0.5 μs for 5 wt.% and 708 ± 1 µs for 10 wt.% TbL10 containing films. A tendency for a reduced life time of the excited state with increasing Tb(III) concentration is observed, which is probably due to partial self quenching occurring to a higher degree at higher Tb(III) concentrations.

3.2.4. Morphology of thin films on glass substrate

AFM images (Figs. 10a,10b) of TbL10/PMMA (7%) nanocomposite films on glass substrate show a smooth, crack-free surface and a uniform microstructure. The section analysis (Fig. 10c) shows that over a horizontal surface distance of about 2 μ m, the surface is smooth, within 1 nm.

3.2.5. Optical properties of thin films on glass substrate

The excitation spectrum (λ_{em} =545 nm) and emission spectrum of TbL10/PMMA film on glass substrate (5 and 10 wt.%) at an excitation wavelength λ_{ex} = 360 nm are shown in Fig. 11. The characteristic bands for the transitions ${}^5D_4 \rightarrow {}^7F_1$ (J=6-3) for Tb(III), equal to those in the pure complex, are observed at the same locations. However, both a decrease of the intensity and broadening of the emission bands at the higher TbL10 concentration is noticeable, guite likely in connection with the residual ligand emission observed. The green light emission observed by the fluorescence microscope (Fig. 11, inset) is evidence that the films possesses good fluorescence. The lifetime of the excited state of TbL10/PMMA glass supported films was found to be 755 \pm 1 μ s at 5 wt.% and 698 \pm 1 µs at 10 wt.% TbL10 containing films. The tendency for reduced life time of the excited state with increasing Tb(III) concentration, observed for the self-supporting films, is also visible here.

The emission spectra of the self-supporting films possess all the emission bands observed in the pure complex, whereas, there are some changes for the glass-supported films. Apparently, the production method has an influence on the emission spectra but it is not critical for the green emission expected.

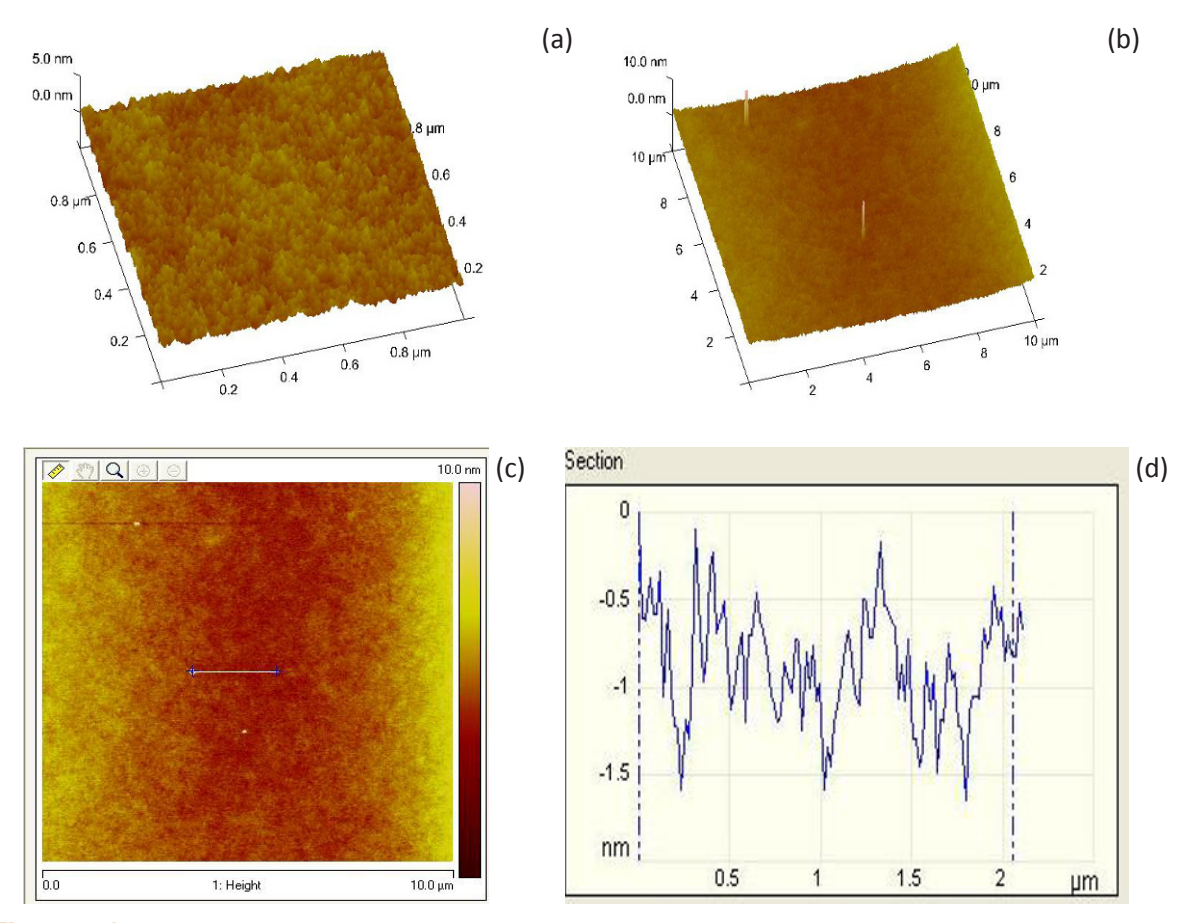


Figure 10. AFM-images of TbL10/PMMA (7 wt.%) nanocomposite films on glass substrate, respectively 1 x 1μm (a) and 10 x 10 μm (b) and AFM section analysis (10 x 10 μm) (c) showing the width and the depth of the surface pores.

4. Conclusions

In the manuscript presented here, the immobilization into PMMA of a newly synthesized luminescent Tb(III) complex is described. The immobilization of Tb(III)-3,3'-[(4-hydroxy)methylene)]bis-(4-hydroxy-2H-1benzopyran-2-one) complex in PMMA-based matrices was successfully performed and nanocomposite films on glass, as well as self-supporting films were obtained. AFM microscope images show a homogeneous and uniform structure of the films. The IR spectra confirm the presence of the complex both in the glasssupported and in self-supporting films. The Tb(III) complex is homogeneously distributed in the matrices. A positive influence of the protective role of the PMMA matrix on the optical properties of the Tb(III) complex was observed: the lifetime of the excited state of the powdered complex (174 µs) and the complex dissolved in ethanol (392 µs) were shorter than that of the immobilized complex in glass supported (755 and 698 µs) and in selfsupporting (761 and 708 µs) PMMA nanocomposite films. The optical properties of

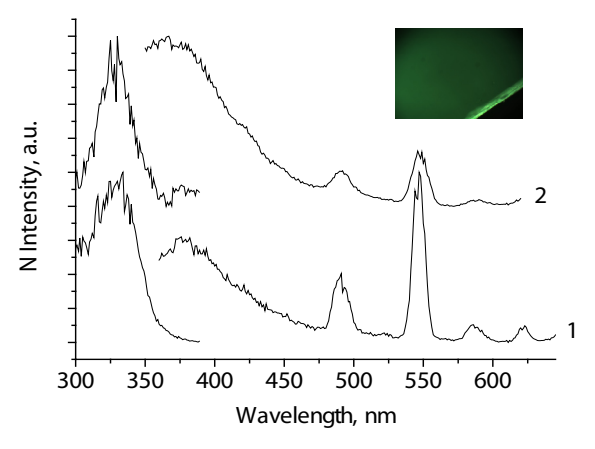


Figure 11. Excitation and emission spectra for glass supported TbL10/PMMA films, 5 (1) and 10 (2) wt.%. The excitation wavelength $\lambda_{\rm sc}$ for the emission spectra was 350 nm. All transitions start from the 5D_4 state and end at the 7F_1 levels (J=6-3).

the Tb(III) ion are preserved in the nanocomposites so the films are highly luminescent, which makes them attractive for the application in green-emitting materials.

Acknowledgement

The financial support of the BG Fund for Scientific Investigations, Project DO 02-129/08, is acknowledged. The quantum yield of the complex was measured in the Laboratory of prof. S. Petoud, CNRS, Orleans, with the financial support of STSM Grant from the COST action CM1006.

References

- [1] Zh. Chen, F. Ding, F. Hao, Z. Bian, B. Ding, Y. Zhu, F. Chen, Ch. Huang, Org. Electronics 10, 939 (2009)
- [2] A. Polman, F.C.J.M. Van Veggel, J. Opt. Soc. Am. B 21, 871 (2004)
- [3] C. Koeppen, S. Yamada, G. Jiang, A.F.J. Garito, Opt. Soc. Am. B 14, 155 (1997)
- [4] J. Kido, Y. Okamoto, Chem. Rev. 102, 2357 (2002)
- [5] M.A. Baldo, M. E. Thompson, S.R. Forrest, Pure Appl. Chem. 71, 2095 (1999)
- [6] Y. Shi, Zh. Deng, J. Xiao, D. Xu, Zh. Chen, R. Wang, J. Luminescence, 122-123, 272 (2007)
- [7] Y. Zhang, Zh. Deng, Ch. Liang, B. Chen, J. Xiao, D. Xu, R. Wang. J. Rare Earths, 24(2), 150 (2006)
- [8] H. Jiu, J. Ding, Y. Sun, J. Bao, Ch. Gao, Qi. Zhang, J Non-Cryst Solids, 352, 197 (2006)
- [9] A.B. Ammann, L. Kölle, H. Brandl, Int. J. Microbiol. 2011, Article ID 435281 (2011) doi:10.1155/2011/435281
- [10] M.A. Bacigalupo, G. Meroni, R. Longhi, Talanta 69(5), 1106 (2006)
- [11] Ga-Lai Law, P. Robert, L.O. Palsson, D. Parker, K.-L. Wong Chem. Commun. 7321 (2009)
- [12] B. Wang, J. Hai, Q. Wang, T. Li, Zh. Yang, Angew. Chem. 50(13), 3063 (2011)
- [13] Z. Ye, M. Tan, G. Wang, J. Yuan, J. Fluoresc. 15(4), 499 (2005)
- [14] J. Ramkumar, Spectrochim. Acta, Part A 65, 993 (2006)
- [15] S. Blair, R. Kataky, D. Parker, New J. Chem 26, 530 (2002)
- [16] J. Kai, M.C.F.C. Felinto, L.A.O. Nunes, O.L. Malta, H.F. Brito, J. Mater. Chem. 21, 3796 (2011)
- [17] J. Zaharieva, M. Milanova, D. Todorovsky, Appl. Surf. Sci. 257, 6858 (2011)
- [18] H. Jiu, L. Zhang, G. Liu, T. Fan, J. Lumines. 129, 317 (2009)
- [19] B. Chen, N. Dong, Q. Zhang, M. Yin, J. Xu, H. Liang, H. Zhao, J. Non-Cryst. Solids 341, 53 (2004)
- [20] X. Chen, B. Yan, J. Optoelectr. Adv. Mater. 8(5), 1931 (2008)

- [21] Y. Li, W. Chian, X. Wang, W. Sha, Y. Zhang, W. Jiang, Photochem. Photobiol. 87(3), 618 (2011)
- [22] Ph. Lenaerts, K. Driesen, R. Van Deun, K. Binnemans, Chem. Mater. 17, 2148 (2005)
- [23] B.D. Wagner, Molecules 14, 210 (2009)
- [24] H. Zhao, N. Neamati, H. Hong, A. Mazumder, S. Wang, S. Sunder, G.W.A. Milne, Y. Pommier, T.R. Burke, J. Med. Chem. 40, 242 (1997)
- [25] A.H. Bedair, N.A. El-Hady, M.S. Abd. El-Latif, A.H. Fakery, A.M. El-Agrody, Il Farmaco 55, 708 (2000)
- [26] I. Kostova, Curr. HIV Res. 4(3), 347 (2006)
- [27] R.E. Gallan, M. Laferriere, J.C. Scaiano, J. Mater. Chem. 16, 1697 (2006)
- [28] K.J. Wallace, R.I. Fagbemi, F.J. Folmer-Andersen, J. Morey, V.M. Lynth, E.V. Anslyn, Chem. Commun. 3886 (2006)
- [29] J. Motoyamagi, T. Fukushima, N. Ishii, T. Aida, J. Am. Chem. Soc. 128, 4220 (2006)
- [30] N. Trendafilova, I. Kostova, V.K. Rastogi, I. Georgieva, G. Bauer, W. Kiefer, J. Raman Spectr. 37, 808 (2006)
- [31] I. Georgieva, N. Trendafilova, W. Kiefer, V.K. Rastogi, I. Kostova, Vibrational Spectr. 44, 78 (2007)
- [32] I. Georgieva, I. Kostova, N. Trendafilova, V.K. Rastogi, W. Kiefer, J. Mol. Structure 979, 115 (2010)
- [33] J. Yao, W. Dou, W. Liu, J. Zheng, Inorg. Chem. Comm. 12, 430 (2009)
- [34] I. Kostova, I. Manolov, I. Nikolova, N. Danchev, II Farmaco 56, 707 (2001)
- [35] I. Kostova, I. Manolov, G. Momekov, Eur. J. Med. Chem. 39, 765 (2004)
- [36] K. Nakamoto, IR Spectra of Inorganic and Coordination Compounds (John Wiley & Sons, New York, 1978)
- [37] M.H.V. Wertz, Science in Progress 88(2), 101 (2005)
- [38] S. Cotton, Lanthanide and Actinide Chemistry (John Wiley and Sons, New York, 2006)